inventions

MDPI

Article

Experimental Analysis for the Use of Sodium Dodecyl Sulfate as a Soluble Metal Cutting Fluid for Micromachining with Electroless-Plated Micropencil Grinding Tools

Peter A. Arrabiyeh [1,*], Martin Bohley [1], Felix Ströer [2], Benjamin Kirsch [1], Jörg Seewig [2] and Jan C. Aurich [1]

[1] Institute for Manufacturing Technology and Production Systems, University of Kaiserslautern, P.O. Box 3049, 67653 Kaiserslautern, Germany; martin.bohley@mv.uni-kl.de (M.B.); benjamin.kirsch@mv.uni-kl.de (B.K.); fbk@mv.uni-kl.de (J.C.A.)

[2] Institute for Measurement and Sensor-Technology, University of Kaiserslautern, P.O. Box 3049, 67653 Kaiserslautern, Germany; stroeer@mv.uni-kl.de (F.S.); seewig@mv.uni-kl.de (J.S.)

* Correspondence: peter.arrabiyeh@mv.uni-kl.de; Tel.: +49-631-205-5483

Received: 29 September 2017; Accepted: 8 November 2017; Published: 10 November 2017

Abstract: Microgrinding with micropencil grinding tools (MPGTs) is a flexible and economic process to machine microstructures in hard and brittle materials. In macrogrinding, cooling and lubrication are done with metal cutting fluids; their application and influence is well researched. Although it can be expected that metal cutting fluids also play a decisive role in microgrinding, systematic investigations can hardly be found. A metal cutting fluid capable of wetting the machining process, containing quantities as small as 0.02% of the water-soluble fluid sodium dodecyl sulfate was tested in microgrinding experiments with MPGTs (diameter ~50 µm; abrasive grit size 2–4 µm). The workpiece material was hardened 16MnCr5.

Keywords: microgrinding; sodium dodecyl sulfate; metal cutting fluid; microstructures; micropencil grinding tools

1. Introduction

Microcomponents with functional surfaces are becoming an integral part [1] in precision industries such as biomedicine, aerospace, microelectronics and telecommunications [2]. There is a growing need for microstructured components, especially ones that manage fluids on the microscopic scale. Microfluidic components generally use a small sample volume, have a good temperature control and can downscale analytical equipment for chemical and biomedical analysis [3].

A number of microstructuring processes have been developed to fulfill the market's need for microstructured components. Processes like LIGA (lithography, electroplating, and molding), micro molding and chemical etching techniques are suitable for the mass production of these parts, but lack the flexibility for small batch production [4]. Micro-end milling [5] and microdrilling are far more suitable for small batch production lines, but are limited in the hardness of machinable materials [4].

In conventional machining, abrasive processes like grinding use superabrasives made of diamonds or cBN (cubic boron nitride) grits to machine hard and brittle materials [6]. In the past, miniaturized versions of these abrasive processes have been developed for microstructuring purposes; among them microgrinding [1]. Microgrinding has a competitive edge over other microstructuring process, since it is used as a finishing process that manufactures surfaces with optical quality while minimizing burr formation [2]. There are two kinds of microgrinding tools in micromachining [4]: thin grinding

wheels called dicing blades used in the semiconductor industry to cut silicon wafers and produce open structures and micropencil grinding tools (MPGTs), used for freeform surfaces and microholes [7].

Microgrinding is a process in which the material removal takes place by stochastically distributed grits [8]. The grits have different protrusions, resulting in material removal at different chip thicknesses. The value of the chip thickness needs to surpass a minimal size to initiate material removal, otherwise only elastic and plastic deformation occur during the machining process. Most grits do not reach that minimal chip thickness, resulting in very high local temperatures due to friction [9]. High temperatures in turn can cause intense tool wear and a high thermal strain on the workpiece surface that causes material structure changes and high tensile stresses [9]. A metal cutting fluid (MCF) is needed to improve the surface quality of machined materials to transport the produced chips away from the machining zone and to increase tool life [10].

A typical flood supply of MCF is generally not suitable for micromachining, as a high flow pressure of liquids may influence the tool behavior by applying an additional force [11]. In literature, new lubrication methods and metal cutting fluids have been developed for micromachining processes. Brudek et al. compared the roughness values: the arithmetic mean roughness R_a and the mean roughness depth R_z of micromilled substrates machined with a minimum quantity method to a process where the workpiece is completely immersed in metal cutting fluid. A variety of commercially available MCFs as well as a variety of vegetable oils were used. Both lubrication methods showed similar results with the commercial MCFs having a small edge over the vegetable oils [12]. Nam et al. used nanofluids in a microdrilling process as an alternative to conventional MCFs. Nanofluids are composed by a water- or oil-based fluid containing nanoparticles made of materials like graphite, Al_2O_3, C_{60} or diamond to increase the thermal conductivity and/or decrease friction in the contact area via the ball bearing effect [13]. Pham et al. used another alternative MCF by spraying ionic liquids in a micromilling process while machining aluminum workpieces. Ionic liquids are liquid salts, consisting of an organic cation and an inorganic anion; they have a low vapor pressure, are non-flammable and have a high thermal stability. The test series showed that workpieces machined with ionic fluids reach similar cutting forces and similar roughness values to those machined with commercially available metal cutting fluids [14]. Overall, the impact of MCF in microgrinding is rarely investigated.

The machine tool used in this paper is located in a clean room and is not capsuled to its environment; a metal cutting fluid safe for both the user and the machinery is hence needed for lubrication. Sodium dodecyl sulfate (SDS) is a surfactant and detergent that has lubricating qualities. It is cheap, causes no health hazards and is even commonly used in the soap and shampoo industry [15].

In this paper, MPGTs with a diameter of ~50 µm and a cBN grit size of 2–4 µm are used to machine hardened 16MnCr5 steel using distilled water and minimal quantities of the solid surfactant SDS to lubricate the process. The results are then compared to a dry microgrinding process and one that uses distilled water only as a coolant. Besides the wear and roughness analysis, the paper offers a tool characterization pre- and post-machining, a structure characterization as well as a force analysis.

2. Materials and Methods

2.1. Micropencil Grinding Tools

The substrates used for the MPGTs contain a tungsten carbide content of 92%, a cobalt content of 8% with a grain size of 0.2 µm. The shaft of the substrates has a diameter of 3.175 mm, a bending strength of 4800 N/mm^2 and a Vickers hardness of 1920 $\pm$ 50 HV30 (ISO 3878) [16]. Figure 1 depicts the geometry of a substrate and the two main steps in the manufacturing of MPGTs. A 40° cone is machined on a conventional tool grinding machine onto the substrate to decrease the material removal in the following precision grinding steps. Using a thin grinding wheel, the cylindrical tip of the substrate is machined to have a diameter of 44 $\pm$ 2 µm at a length of 140 µm. For this paper, a grit size of 2–4 µm is used. The tool tip diameter must be readjusted when using different grit sizes with different coating thicknesses to allow the coated tool to reach a diameter of ~50 µm.

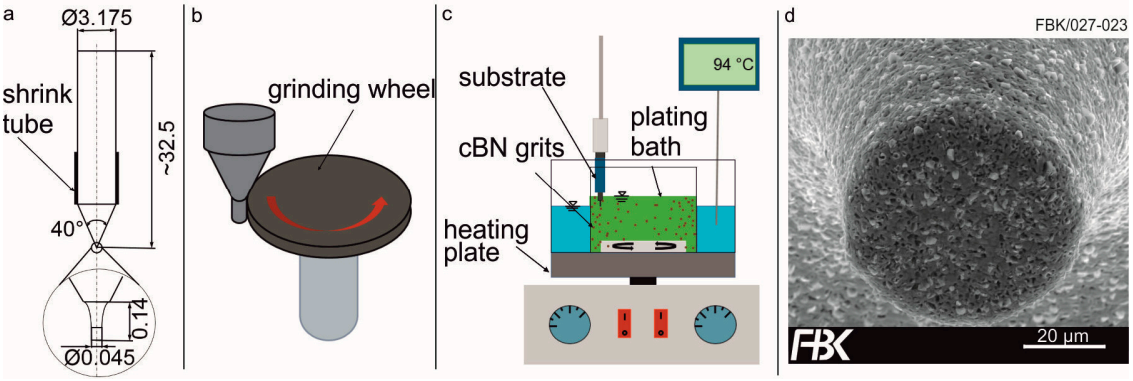

Figure 1. Manufacturing process for micropencil grinding tools (MPGTs): (**a**) geometry of machined substrate; (**b**) microgrinding process for MPGT substrates; (**c**) electroless plating process for MPGT and (**d**) finished MPGT with 2–4 µm grit size.

Following the machining process, the substrate is degreased in an alkaline degreasing solution, which is then neutralized in a hydrochloric acid solution. Then a thin nickel layer is electroplated onto the substrate (Figure 2) to provide an active, chemically affine nickel surface. Shrink tubes are applied to the substrates as a resist to limit the nickel coating to a defined area [17]. Finally, the electroless-plating process is performed.

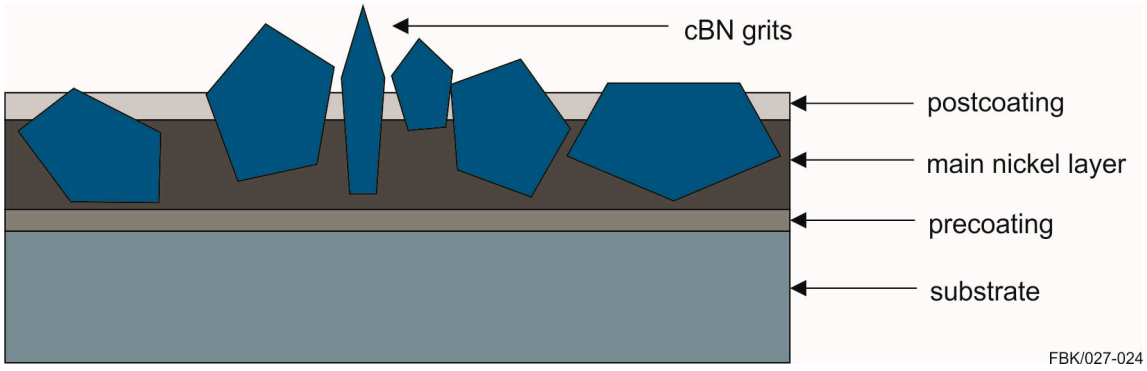

Figure 2. Abrasive layer. cBN: cubic boron nitride.

Electroless plating is a process that is based on the principle of ionic reduction. In the solution, a metal salt, in this case nickel sulfate, provides the solution with Ni^{2+} free nickel ions. A reducing agent like sodium hypophosphite can provide the nickel ions with the two missing electrons, slowly forming a phosphorous nickel coating onto an active surface; the components of the plating solution are listed in Table 1. The process is suited to manufacture small quantities of MPGTs, with flexible, custom design choices in regards to its form, diameter, coating thickness, grit size, grit concentration and grit protrusion [17].

Using the ingredients listed in Table 1, a quantitative energy dispersive X-ray (EDX) analysis shows that a phosphorous content of 6.01% $\pm$ 0.55% can be achieved. A phosphorus content of less than 7% results in a face-centered cubic crystal structure, while an amorphous structure is produced at higher phosphorus contents [18]. A low phosphorous content generally produces a harder nickel layer [19].

Table 1. Electroless-plating solution composition [20].

Component	Concentration in g/L
Nickel sulfate ($NiSO_4 \cdot 6H_2O$)	30
Sodium hypophosphite (NaH_2PO_2)	20
Sodium acetate ($C_2H_3NaO_2$)	20
Thiourea (CH_4N_2S)	0.0004
Hydrochloric acid (HCl)	Adapted to a pH value of 5.2–5.4
cBN grits	4

The abrasive grits are whirled up in the coating solution via a magnetic stirrer. The main coating time for a monolayered MPGT is 150 s for a grit size of 2–4 µm. After the main coating time, the magnetic stirrer stops and the grits fall to the bottom of the beaker, allowing to embed the grits on the MPGT with an additional nickel layer for 90 s (see Figure 2). The final product for a single layered MPGT can be seen in Figure 1d. Using scanning electron microscopy (SEM) images and an image processing software, a quantitative analysis was conducted to determine the grit concentration on the tool. A grit concentration of 35% ± 7% was found.

2.2. Experimental Setup

The results presented in the following chapters were produced on a high precision three-axis machine tool (Figure 3) mounted on top of a vibration isolated granite plate. The tool spindle is mounted vertically onto the *z*-axis on a cross-roller bearing stage. Rotation speeds in the range of 5000–54,000 rpm can be achieved. The X–Y table is guided by air bearings and can move with a positioning accuracy of <1 µm [5]. A Kistler 3-component dynamometer (9119AA1) dynamometer for measuring cutting forces is mounted on top of the X–Y table; the workpieces are clamped onto the dynamometer.

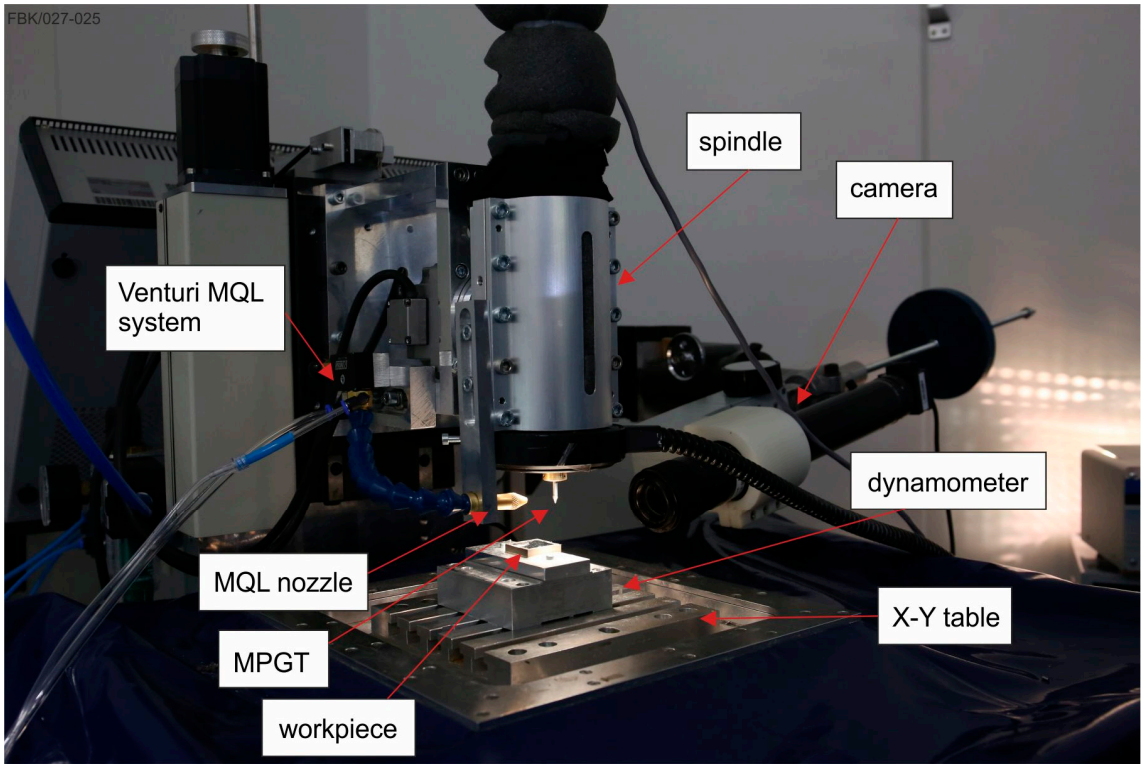

Figure 3. Machine tool for microgrinding and milling. MQL: minimum quantity lubrication.

A Venturi minimum quantity lubrication (MQL) system is used to spray the machining process with an air/liquid mixture. By narrowing the cross-section at the nozzle head, a pressure difference is created through which the liquid is suctioned. The air acts as a transport medium for the liquid. Flow rates of <100 mL/h are defined as MQL in macro machining. However, considering the small sizes of tools and structures and the comparably low material removal rates in microgrinding, 100 mL/h can be defined as flood cooling in microgrinding.

Images of the tools and their respective structures were captured using a scanning electron microscope (SEM). The structures were analyzed using a confocal microscope (Nanofocus µsurf) with a 60× magnification lens and a numerical aperture (NA) of 0.9.

2.3. Experimental Procedure

To test the influence of SDS as a metal cutting fluid in the microgrinding process, MPGTs with diameters ~50 µm were used to machine 500 µm long grooves into hardened 16MnCr5 (SAE5115; 665 HV30 ± 15 HV30 (according to ISO 6507 [21])). The workpiece was face-machined with a larger pencil grinding tool (diameter = 3.175 mm) to compensate for assembly-related influences and to gain a flat surface. To test the effect of the soluble lubricant, a small amount of 0.2 g/L was added to a distilled water medium and was used for the experiments. For comparison, the microgrinding process was also conducted dry and with distilled water as metal cutting fluid. Both the SDS and distilled water experiments were conducted with a volume flow rate of 60 ± 10 mL/h and a positive air pressure of 0.65 bar. Both form a fluid film around the tool during the process (Figure 4b); experiments showed that if the fluid film is interrupted, immediate damage to the abrasive layer occurs.

Based on preliminary studies; a rotation speed of 30,000 rpm (cutting speed of 4.71 m/min) was applied. Feed rates of 0.05 mm/min and 0.1 mm/min were used at a depth of cut of 5 µm; Figure 4a shows the parameter combinations studied in this paper with each combination being repeated three times. The tools were maneuvered to the starting position optically using the camera. The MPGT is used to scratch the surface of the workpiece to determine the zero position between tool and workpiece. This results into a positioning accuracy of ±50 µm and hence in an according deviation of the groove length. The tool rotates in clockwise direction, while the workpiece was given a feed rate towards the tool.

a

case	feed rate in mm/min	rotational speed in rpm	metal cutting fluid
case 1	0.05	30,000	dry
case 2	0.1	30,000	dry
case 3	0.05	30,000	water
case 4	0.1	30,000	water
case 5	0.05	30,000	SDS
case 6	0.1	30,000	SDS

b

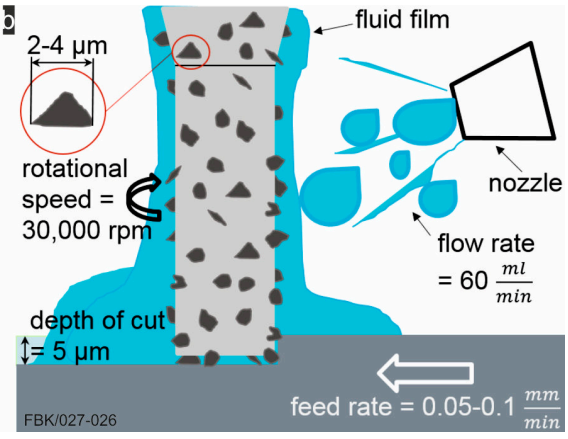

Figure 4. (**a**) Microgrinding test series; (**b**) microgrinding process.

3. Results

3.1. Tool Wear

Figure 5 visualizes the tool wear for four of the parameter combinations (cases) listed in Figure 4a; the results from parameter combination 2 and 4 were left out of the figure, because they do not differ

from cases 1 and 3. The tools used in the dry machining process lose their abrasive layer on the face side of the tool upon entry (Figure 5a). The abrasive layer breaks off the MPGT and rips part of the layer on the circumference of the tool as well (Figure 5a). It is assumed that high temperatures occur on the face side of the MPGT due to friction. Tungsten carbide with an 8% cobalt content has a linear thermal expansion coefficient of 5×10^{-6}–5.2×10^{-6} K^{-1} which is much smaller than that of nickel which lies in a range of 12×10^{-6}–13.5×10^{-6} K^{-1} [22]. Thus, the abrasive layer expands much more with rising temperature than the substrate, causing the abrasive layer to loosen up until the process forces eventually result into failure of the abrasive layer.

MPGTs cooled with water showed a slight improvement over the ones used in dry machining, despite losing the abrasive layer. The tools had a longer tool life than the ones used in dry machining as can be seen from the abrasive layer breakoff point presented in Figure 5b. The abrasive layer stays in tact in both cases that use SDS for lubrication (Figure 5c,d); except for one tool used in case six that broke off 10 µm before finishing its groove. Tool wear is slightly higher for case 6 due to the increase in feed rate.

An energy-dispersive X-ray analysis (EDX) was performed to determine the iron adhesion on the face side of the abrasive layer and the nickel adhesion at the bottom of the structure. While the analysis showed no signs of nickel adhesion in the structure, an iron concentration of 28.65% ± 5.1% for case 5 and 50.05% ± 0.78% for case 6 was identified. The results are qualitative and require further investigation; however, a direct relationship between feed rate and material adhesion could be determined. According to Klocke, adhesions that fill the chip space, increase friction, and therefore the process temperature and the process forces. Material adhesions increase the wear of the machining tool by breaking out single grits or even entire grit populations [9].

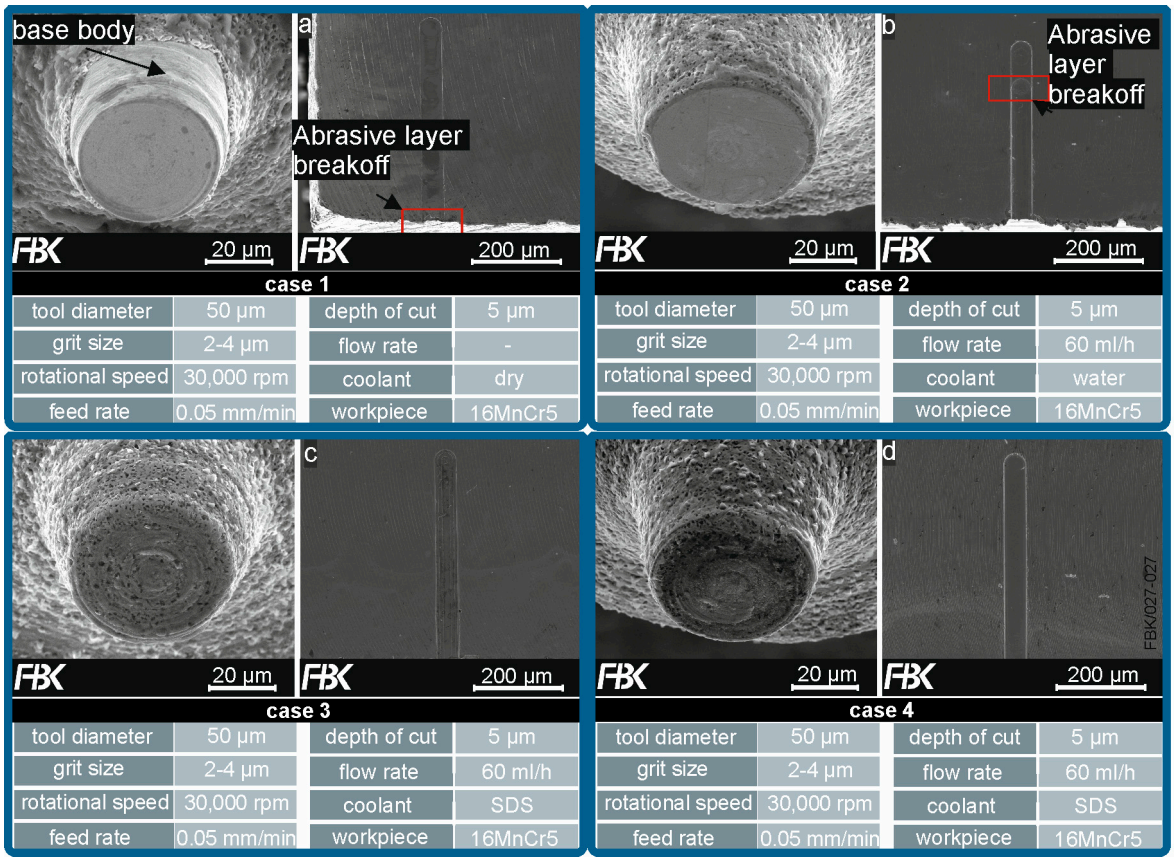

Figure 5. MPGTs post-microgrinding: (**a**) case 1; (**b**) case 3; (**c**) case 5 and (**d**) case 6.

3.2. Structure Analysis

Topographies of the structures machined with all six parameter combinations were measured using a confocal microscope (Nanofocus µsurf) with a 60× magnification lens and a numerical aperture of NA = 0.9. Multiple measurements were combined using the stitching algorithms integrated in the measurement devices software. Missing data points, resulting from the finite numerical aperture or artefacts on the surfaces, were interpolated using linear interpolation. A first order plane levelling minimizing the sum of the squared distances was applied to the areal measurement data. Profiles located in the center of the groove with a length of 400 µm were extracted manually from the areal data. Calculation of 2D roughness parameters included limitation of the bandwidth using the Gaussian-filter [23,24] (l_c = 80 µm; l_s = 0 µm).

To estimate the surface quality, the mean roughness depth R_z and the arithmetical mean roughness value R_a [25], were calculated according to DIN EN ISO 4288. According to the ISO standard, five consecutive 80 µm long segments (from a 400 µm long section) were used to calculate the roughness R_{ai} with i = 1, . . . , 5 of a structure [26], with the first segment starting at the entry point of each groove, in order to monitor the tool right from the start.

Figure 6a,b display the mean values of R_a and R_z for all six parameter combinations with their respective standard deviations. A few trends are visible in the diagrams; the first being that grooves machined with lubrication (Cases 5 and 6), resulted in the smallest roughness values, while grooves machined dry exhibited overall higher values. The standard deviation of the roughness parameters is also much smaller for grooves machined with the SDS mixture, which is synonymous for a more stable process, since less material adhesion on the slot bottom appeared. Another visible trend is that grooves machined with a feed rate of 0.1 mm/min feature smaller roughness values when compare to those machined with a 0.05 mm/min feed rate which is a surprising trend considering higher uncut chip thicknesses at higher feed rates. The lower roughness at higher feeds could be led back to the higher tool wear and higher material adhesion at larger feed rates.

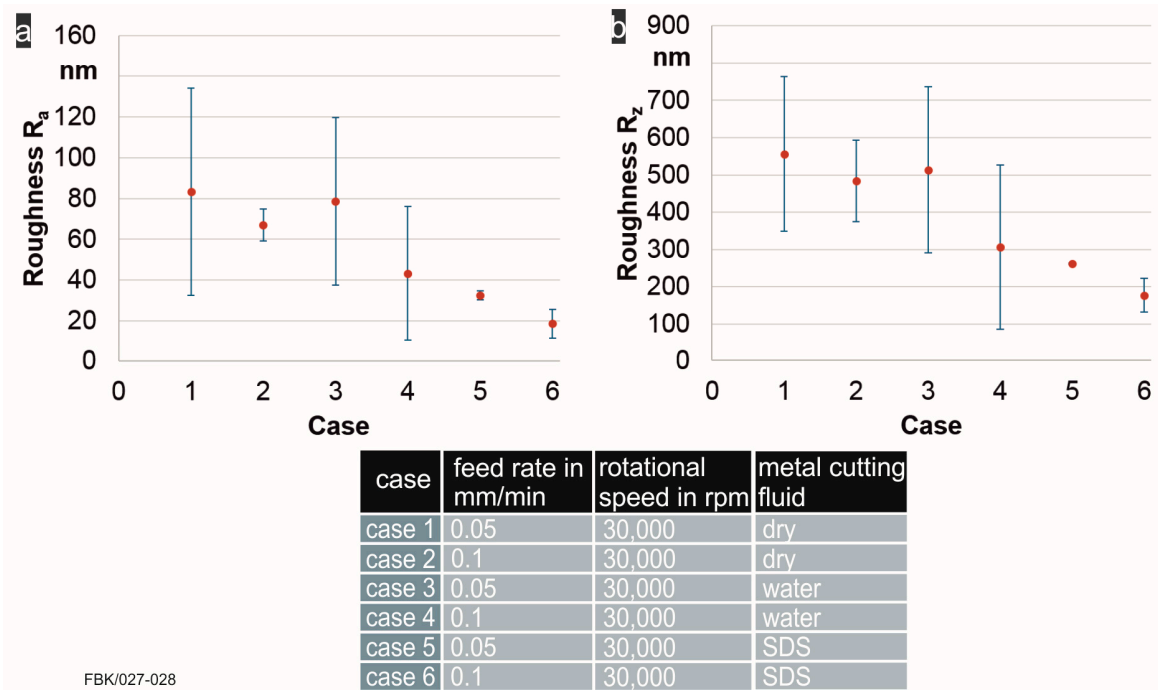

case	feed rate in mm/min	rotational speed in rpm	metal cutting fluid
case 1	0.05	30,000	dry
case 2	0.1	30,000	dry
case 3	0.05	30,000	water
case 4	0.1	30,000	water
case 5	0.05	30,000	SDS
case 6	0.1	30,000	SDS

Figure 6. (**a**) Roughness values R_a and (**b**) Roughness values R_z.

The sample structure presented in Figure 7c is one of the structures from case 6. It is chosen to present some of the more prominent tool-specific and structural characteristics. The first being the

obvious breakoff at the entry point—this indicates a loss in abrasive grits. Judging from Figure 7a, many grits at the center of the tool had a rather high protrusion; some of these grits broke off upon entry due to a lack of grit retention forces at small high grit protrusion and at the same time high uncut chip thickness, resulting in high loads on those grits. A small 9 µm broad smaller groove in the middle of the structure (Figure 7c) suggests that the grits at the center of the tool had a higher protrusion. Figure 7b shows the tool after the machining process and a small circular marking off the pivot of the tool, which coincidently measures to 9 µm. This pivot is located 2.5 µm off the center of the tool, hence a reclamping error occurred, producing a step-like structure at the right side of the groove (Figure 7c). This difference in cutting depths can be led back to a difference in height for parts of the abrasive layer; this difference in height is marked in Figure 7b but can also be seen in Figure 7a (less grit protrusion). One final, more common characteristic is the material adhesion to the bottom of the groove, on the up grinding side.

The manifestation of these characteristics is unique to each individual MPGT. Some of them can be prevented by sorting out tools that have a higher variation in grit protrusion; however, due to constant wear, the grits are exposed to during the machining process—it is impossible to prohibit them completely.

The groove analyzed in in Figure 7c was machined with SDS and a feed rate of 0.1 mm/min. Different from other structures machined with SDS, the structure has a large material adhesion at the bottom surface; a characteristic more commonly observed with those machined dry. The structure in Figure 7c shows almost no signs of burrs and only few, small chippings, while cases 1–4 show much larger and frequent burr and chipping formations because no material cutting happens after the loss of an abrasive layer. An example of a dry machined structure is shown in Figure 8.

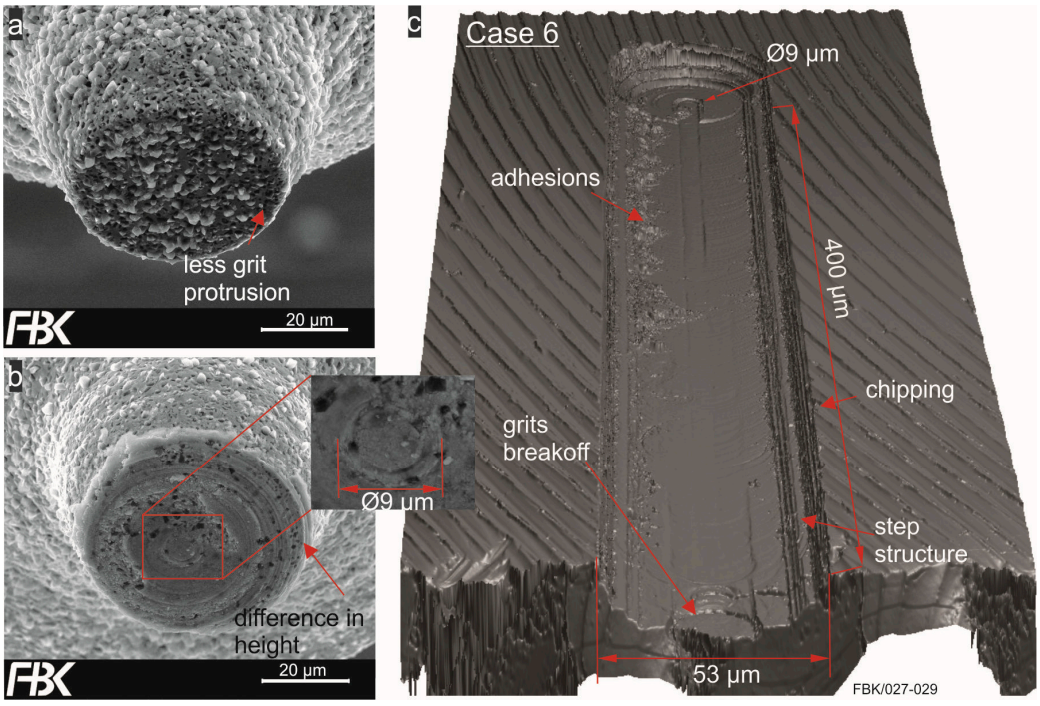

Figure 7. (**a**,**b**) Tool that machined the groove sample, before and post machining and (**c**) sample of a structure machined with sodium dodecyl sulfate (SDS) and a feed rate of 0.1 mm/min, measured by confocal microscopy.

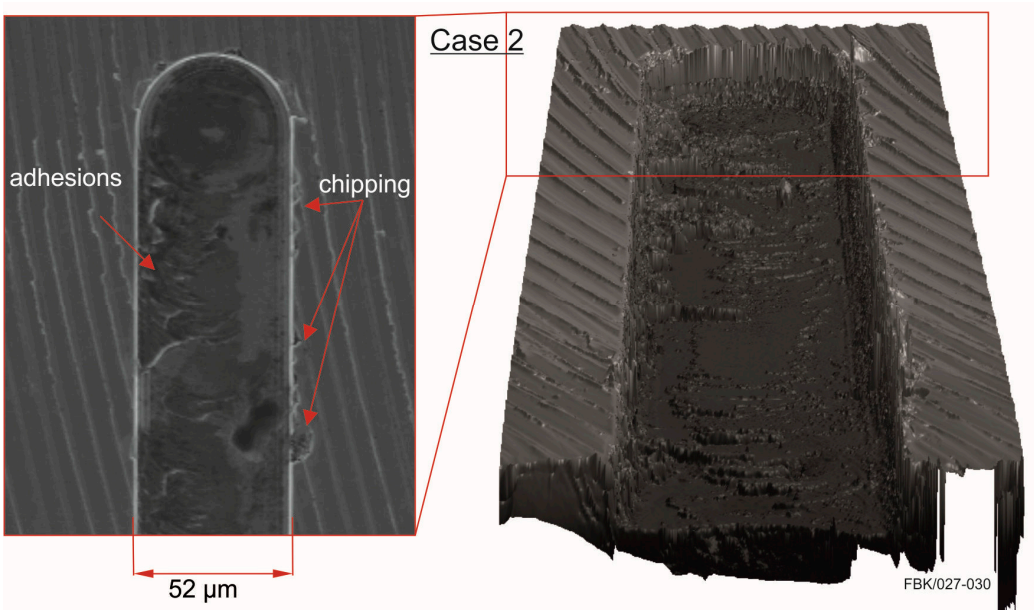

Figure 8. Sample of a dry machined structure with a feed rate of 0.1 mm/min, measured by confocal microscopy. A segment is shown with scanning electron microscopy (SEM).

3.3. Force Measurements

The process forces were measured with a Kistler 3-component dynamometer (9119AA1) during machining. The sampling rate was 10 kHz for all grinding parameters.

After recording, the data was evaluated with National Instruments Software DIAdem. With the help of a fast Fourier transformation, the actual spindle speed was determined. With this information a bandpass filter was applied to extract and consider the frequencies in the signal corresponding to the spindle speed ±20 Hz only. Thus, not the actual process forces were used for this research but the dynamic process characteristics evaluated and compared. The reason for this configuration is the use of metal cutting fluid. The impact of the fluid application on the workpiece was higher than the impact of the cutting process itself.

Figure 9 shows one of the grooves machined for case 4 to demonstrate the correlation between forces and depth of cut. In Section 1, where the tool is starting to cut the material, the force rates are rising until the complete tool diameter is in contact. This area is followed by Section 2, where the cutting conditions seem to be unstable. The cutting forces as well as the feed forces start to rise and show sharp peaks. At a feed travel of about 150 µm, the forces reach their maximum and some abrasive grits broke out of the layer or parts of the layer itself broke out, which can be seen in the confocal image, showing a difference in the resulting geometry of the slot bottom. Until a feed travel of 250 µm (Section 3), the surface as well as the force amplitudes show an unstable behavior. The depth of cut is changing in two steps. Until the end of the slot at 500 µm, the force levels as well as the slot bottom geometry are at a stable cutting regime. At the end of Section 4, the force levels are falling abruptly after the feed of the machine tool is being stopped.

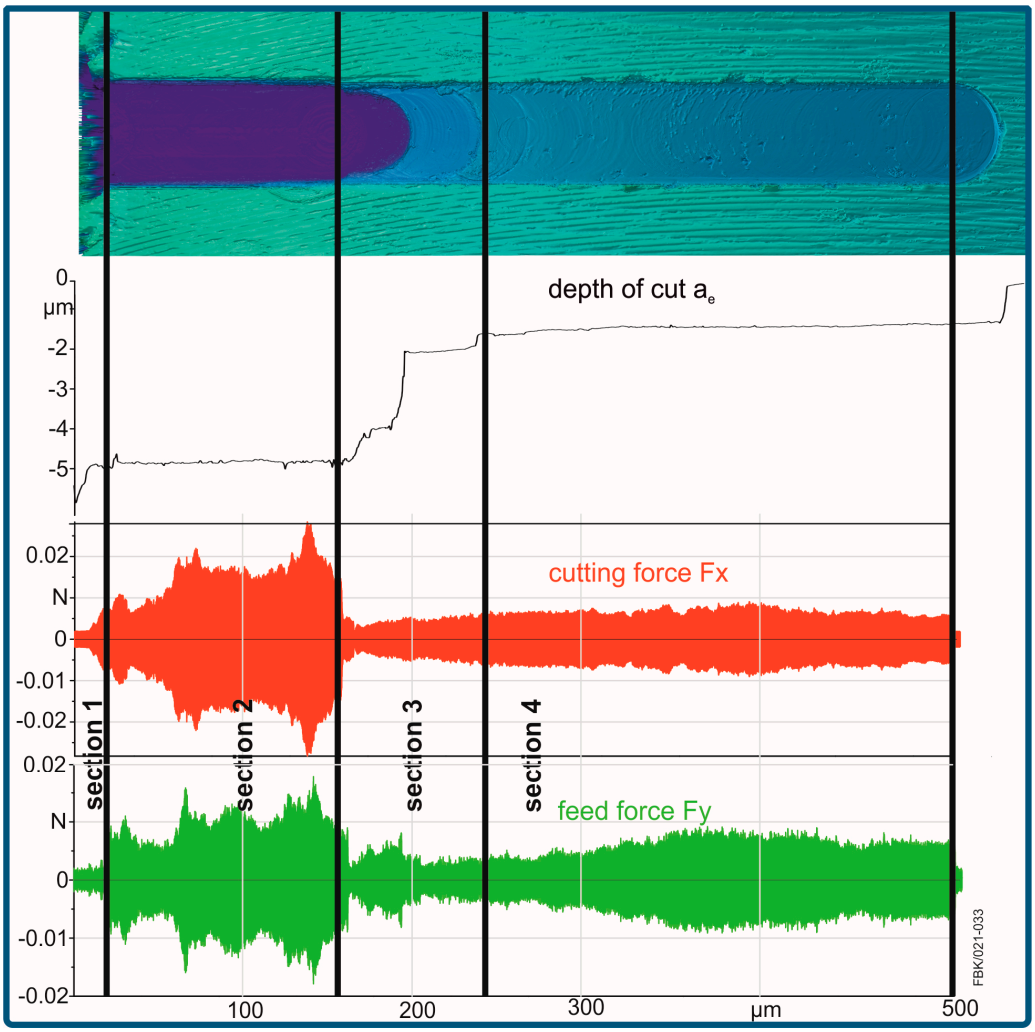

Figure 9. Comparison of slot bottom geometry and the equivalent force levels.

4. Conclusions and Outlook

Microgrinding is a process in which a very high amount of rubbing and ploughing occurs. This can result in high temperatures, high wear of the tools and ultimately a low quality of the machined structures. This paper presents a systematic investigation on the influence of the application of metal cutting fluids on tool wear and structure quality.

The application of a new metal cutting fluid (MCF), consisting of small quantities (0.02% in distilled water) of the solid lubricant sodium dodecyl sulfate (SDS) was tested when microgrinding. In this test series, microgrinding experiments with monolayered electroless plated micropencil grinding tools (diameter ~50 µm and grit size 2–4 µm) were conducted to analyze the effect of the new metal cutting fluid. The results were compared to pure distilled water and dry machining experiments at a rotational speed of 30,000 rpm and the two-feed rate variations of 0.05 mm/min and 0.1 mm/min.

The results showed that the micropencil grinding tools (MPGTs) used in dry machining and with distilled water were unable to complete a 500-µm long groove without losing part of their abrasive layer. In contrast, the grooves machined with SDS were completed with the tool intact.

The structures were analyzed using a confocal microscope. Both the roughness values and the structure characteristics were examined. Highest roughness values were measured for the dry grinding cases and lowest roughness values for cases machined with SDS. Besides the lower roughness, a more stable process was achieved with the application of SDS. This was manifested by small standard

deviations of the roughness values. The application of SDS also resulted into less burr formation and chipping, as well as less adhesions on the bottom surface.

In conclusion, the results revealed that the process stability and the quality of the machined structures is highly influenced by the application of metal cutting fluids. Future work will hence deal with the investigation of the flow rate and the SDS concentration. In addition, tool and machining parameter case studies are required to explore the possibilities and limitations of increasing both the tool life and the productivity of the process. A further analysis of structure and tool characteristics will be conducted to get a better understanding of the tool wear characteristics and their influence on the structures.

Acknowledgments: This research was funded by the German Research Foundation (DFG) within the Collaborative Research Center 926 "Microscale Morphology of Component Surfaces"—through the subproject B09 "Geometrical Structuring of Component Surfaces by Microgrinding".

Author Contributions: Peter A. Arrabiyeh has conceived, designed, performed and documented the microgrinding and electroless plating experiments. Peter A. Arrabiyeh, Martin Bohley and Felix Ströer conducted the structural analysis of machined microstructures. Martin Bohley analyzed the data collected from the dynamometer. Peter A. Arrabiyeh conducted SEM and EDX analysis. Benjamin Kirsch supervised the present study and helped to discuss and analyze the results. Jan C. Aurich initiated the study. All authors were highly involved in writing the paper.

Conflicts of Interest: The authors declare no conflicts of interest.

References

1. Feng, J. Microgrinding of Ceramic Materials. Ph.D. Thesis, Michigan Technological University, Houghton, MI, USA, 2010.
2. Pratap, A.; Patra, K.; Dyakonov, A.A. Manufacturing miniature products by micro grinding: A review. *Procedia Eng.* **2016**, *150*, 969–974. [CrossRef]
3. Wensink, H. Fabrication of Microstructures by Powder Blasting. Ph.D. Thesis, University of Twente, Enschede, The Netherlands, 2002.
4. Engmann, J. *Galvanisch Gebundene Mikroschleifstifte. Entwicklung, Herstellung und Einsatz, Als Ms. Gedr*; Produktionstechnische Berichte aus dem FBK 01/2011; Technischen Universität Kaiserslautern: Kaiserslautern, Germany, 2011.
5. Reichenbach, I.G.; Aurich, J.C. Untersuchung der oberflächengüte beim mikrofräsen—einfluss von prozessparametern und einstellwinkel der nebenschneide bei 48 µm mikroschaftwerkzeugen. *Wt Werkstattstechnik Online* **2013**, *103/11–12*, 847–852.
6. Brinksmeier, E.; Mutlugünes, Y.; Klocke, F.; Aurich, J.C.; Shore, P.; Ohmori, H. Ultra precision grinding. *CIRP Ann. Manuf. Technol.* **2010**, *59*, 652–671. [CrossRef]
7. Hoffmeister, H.-W.; Hlavac, M. Schleifen von Mikrostrukturen. In *Tagungsband des 10. Feinbearbeitungskolloqiums in Braunschweig*; Vulkan-Verlag: Essen, Germany, 2002; pp. 7.1–7.24.
8. Setti, D.; Sinha, M.K.; Ghosh, S.; Rao, P.V. Performance evaluation of Ti–6Al–4V grinding using chip formation and coefficient of friction under the influence of nanofluids. *Int. J. Mach. Tools Manuf.* **2015**, *88*, 237–248. [CrossRef]
9. Klocke, F. *Manufacturing Processes 2: Grinding, Honing, Lapping*; Springer: Berlin, Germany, 2009.
10. Brinksmeier, E.; Heinzel, C.; Wittmann, M. Friction, cooling and lubrication in grinding. *CIRP Ann. Manuf. Technol.* **1999**, *48*, 581–598. [CrossRef]
11. Dornfeld, D.; Min, S.; Takeuchi, Y. Recent advances in mechanical micro-machinability of copper 101 using tungsten carbide micro-end mills. *Int. J. Mach. Tools Manuf.* **2006**, *55*, 745–768.
12. Brudek, G. *Beiträge zur Prozessanalyse in der Mikrozerspanung. Insbesondere für das Mikrofräsen*; Berichte aus dem Institut für Konstruktions- und Fertigungstechnik Bd. 8; Shaker: Aachen, Germany, 2007.
13. Nam, J.S.; Kim, D.H.; Chung, H.; Lee, S.W. Optimization of environmentally benign micro-drilling process with nanofluid minimum quantity lubrication using response surface methodology and genetic algorithm. *J. Clean. Prod.* **2015**, *102*, 428–436. [CrossRef]
14. Pham, M.Q.; Yoon, H.S.; Khare, V.; Ahn, S.H. Evaluation of ionic liquids as lubricants in micro milling-process capability and sustainability. *J. Clean. Prod.* **2014**, *76*, 167–173. [CrossRef]

15. Smulders, E.; Rybinski, W.-V.; Sung, E.; Rähse, W.; Steber, J.; Wiebel, F. *Nordskog: Ullmann's Encyclopedia of Industrial Chemistry*; Wiley-VCH Verlag GmbH & Co. KGaA: Weinheim, Germany, 2000.
16. *DIN EN ISO 3878, Hardmetals, Vickers Hardness Test, Identical with ISO 3878:1983*; International Organization for Standardization: Geneva, Switzerland, 1991.
17. Arrabiyeh, P.A.; Kirsch, B.; Aurich, J.C. Development of micro pencil grinding tools via an electroless plating process. *J. Micro Nano Manuf.* **2017**, *5*, 011002. [CrossRef]
18. Lin, K.L.; Hwang, J.W. Effect of thiourea and lead acetate on the deposition of electroless nickel. *Mater. Chem. Phys.* **2002**, *76*, 204–211. [CrossRef]
19. Mallory, G.O.; Hajdu, J.B. *Electroless Plating: Fundamentals and Applications*; American Electroplaters & Surface Finishers Society: Orlando, FL, USA, 1990.
20. Kirsch, B.; Bohley, M.; Arrabiyeh, P.A.; Aurich, J.C. Application of ultra-small micro grinding and micro milling tools: Possibilities and limitations. *Micromachines* **2017**, *8*, 261. [CrossRef]
21. *DIN EN ISO 6507-1:2006-03 Metallic Materials—Vickers Hardness Test—Part 1: Test Method*; International Organization for Standardization: Geneva, Switzerland, 2006.
22. Granta Design Ltd. *CES EduPack Software*; Granta Design Ltd.: Cambridge, UK, 2012.
23. *DIN EN ISO 16610-21:2013-06 Geometrical Product Specifications (GPS)—Filtration—Part 21: Linear Profile Filters: Gaussian Filters*; International Organization for Standardization: Geneva, Switzerland, 2012.
24. *DIN EN ISO 11562:1998-09 Geometrical Product Specifications (GPS)—Surface Texture: Profile Method—Metrological Characteristics of Phase Correct Filters*; International Organization for Standardization: Geneva, Switzerland, 1997.
25. *DIN EN ISO 4287:2010-07 Geometrical Product Specifications (GPS)—Surface Texture: Profile Method—Terms, Definitions and Surface Texture Parameters*; International Organization for Standardization: Geneva, Switzerland, 2009.
26. *DIN EN ISO 4288:1998-08 Geometrical Product Specifications (GPS)—Surface Texture: Profile Method—Rules and Procedures for the Assessment of Surface Texture*; International Organization for Standardization: Geneva, Switzerland, 1997.

© 2017 by the authors. Licensee MDPI, Basel, Switzerland. This article is an open access article distributed under the terms and conditions of the Creative Commons Attribution (CC BY) license (http://creativecommons.org/licenses/by/4.0/).